CHEMISTRY OF MATERIALS

pubs.acs.org/cm

Article

Dynamic Chiral PPA–AgNP Nanocomposites: Aligned Silver Nanoparticles Decorating Helical Polymers

Manuel Núñez-Martínez, Sandra Arias, Emilio Quiñoá, Ricardo Riguera, and Félix Freire*

Cite This: *Chem. Mater.* 2021, 33, 4805–4812

Read Online

ACCESS | Metrics & More | Article Recommendations | Supporting Information

ABSTRACT: A novel approach to prepare stimulus-sensitive nanocomposites is described, based on a dynamic helical polymer, chiral poly(phenylacetylene) (PPA), and silver nanoparticles. To preserve the dynamic helical behavior of PPA within the nanocomposite, a weak and adaptive supramolecular interaction, such as that between amide group–silver nanoparticle, is used to link the metal nanoparticle to the polymer. To prepare the composite, we chose PPA as a helical polymer that bears an amide group as a monomer repeating unit, poly-(*R*)-**1**, which can coordinate with Ag^+ ions. The silver ions that form complexes with the pendant groups are further reduced, through the use of $NaBH_4$, to AgNPs that are stabilized by the amide groups of PPA. As a result, 2.8 nm silver nanoparticles are formed and aligned along the polymer chain with a regular 3.1 nm interparticle distance corresponding to the helical pitch of the polymer. The weak amide/AgNP interactions allow PPA to adopt either *P* or *M* helical structures on the AgNPs through supramolecular adaptive mechanisms induced by appropriate external stimuli.

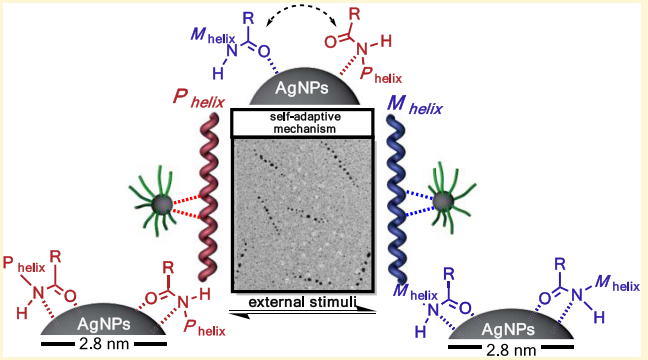

INTRODUCTION

Among many relevant characteristics, metallic nanoparticles (MNPs) have also attracted the attention of the scientific community due to their optical properties related to the presence of localized surface plasmon resonance (LSPR) bands,[1,2] which find applications in different fields such as theranostics,[3] colorimetric sensors,[4] drug delivery,[5,6] and surface Raman scattering (SERS)[7−9] among others.

One of the main problems of MNPs is their high aggregation tendency. To avoid this problem, scientists have coated the surface of the MNPs with a large variety of molecules to stabilize them by either steric or electrostatic effects. This stabilization can be also achieved using polymers or macromolecules as coating agents. In such cases, the resulting hybrid materials conserve the properties of the MNP, as well as those derived from the polymeric coating, such as stability, solubility, and biocompatibility.[1,10]

In the case of using DNA or proteins as coating agents to stabilize the MNP,[1] the biological function of the hybrid material is related to the helical structure adopted by the macromolecule. Interestingly, just a couple of nanocomposites are reported using that use a non-natural helical coating such as a synthetic polymer or a foldamer rather than a biomacromolecule.[11−14] In this sense, derivatization of MNPs with synthetic dynamic helical polymers such as poly(acetylene)s (PAs), poly(phenylacetylene)s (PPAs), or poly(diphenylacetylene)s (PDPAs) should represent a clear advantage because their helical senses (*P*/*M*) and/or chain elongations (compression/stretching) are not fixed as in the biomacromolecules, and can be tuned through the action of external stimuli.[15−24]

During the last years, some attempts have been made to create nanocomposites based on dynamic helical polymers and metal nanoparticles using thiolated pendant groups.[11−14] These studies showed that the dynamic behavior of the helical polymer is dramatically affected by the presence of a thiolated monomer, where the stimuli-response properties of the nanocomposite are reduced up to 20%. To circumvent that problem, a different approach to link the MNP to PPA must be inspected.

In this case, we look for weaker supramolecular interactions between PPAs and MNPs, such as those present in PVP–AgNPs and PVP–AuNPs, where poly(vinylpyrrolidone) (PVP) provides the amide groups required for the stabilization.[25−27] Thus, in this work, we decided to stabilize AgNPs with dynamic PPA[28−37] bearing amide groups in the pendants (Scheme 1). In such a case, a self-adaptive mechanism of helical inversion or helical enhancement is expected, where a

Received: March 8, 2021
Revised: May 4, 2021
Published: May 12, 2021

https://doi.org/10.1021/acs.chemmater.1c00805
Chem. Mater. 2021, 33, 4805–4812

Scheme 1. Preparation of Hybrid PPA−MNPs Using Supramolecular Amide/PPA−MNP Interactions

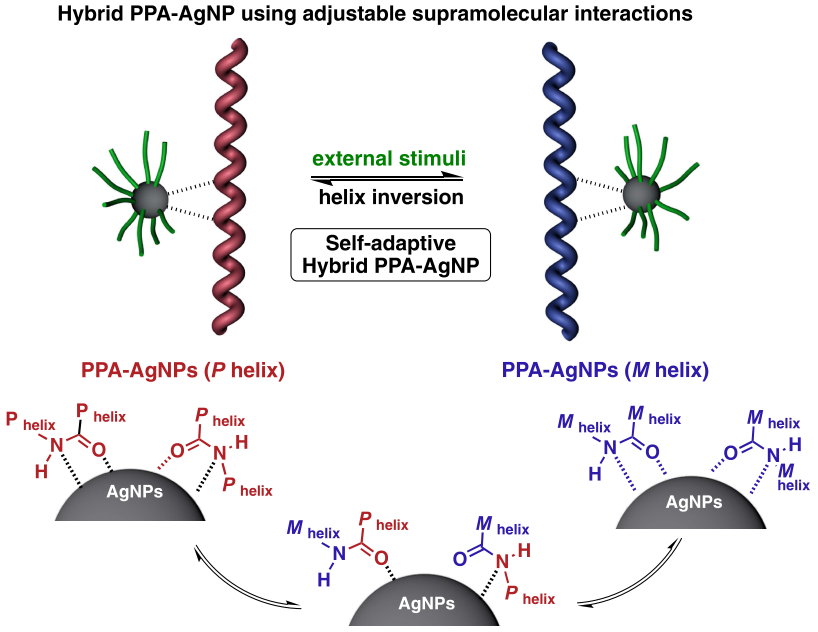

part of the weak supramolecular interactions between the amide groups and the metal nanoparticles are disrupted during the helical structural change, sense and/or elongation. These interactions recover immediately afterward (Scheme 1), thus producing the same structural changes in the PPA−AgNP chain that occur in the isolated PPA.

RESULTS AND DISCUSSION

To perform these studies, two well-known PPAs were chosen as model compounds: poly-(*R*)-**1** that bears 4-anilide of (*R*)-*α*-methoxy-*α*-phenylacetic acid and poly-(*R*)-**2** that bears 4-anilide of (*R*)-*α*-methoxytrifluoromethylphenylacetic acid (Figure 1). In both cases, an amide group is present in the monomer repeating unit. These PPAs were prepared according to previous studies using $[Rh(nbd)Cl]_2$ as a catalyst (nbd = 2,5-norbornadiene) (see the Supporting Information).[18]

These two polymers, poly-(*R*)-**1** and poly-(*R*)-**2**, were selected taking into account their different dynamic helical behaviors and the distinct donor character of the amide group at the pendant.

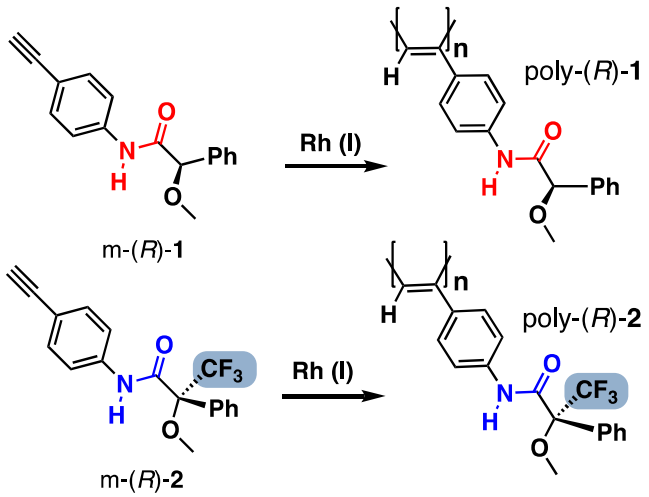

Figure 1. Chemical structures of monomers and polymers used in this work.

Thus, poly-(*R*)-**1** is a highly dynamic helical polymer and, in the absence of external stimuli, exists as an axially racemic polymer, equal populations of *P* and *M* helices, which can selectively adopt a preferred *P* or *M* helicity when divalent or monovalent metal ions are added as external stimuli to a solution of the polymer.[18,38,39] On the other hand, poly-(*R*)-**2** is also a dynamic helical polymer, whose elongation and helical sense are affected by the donor and polar characters of the solvent used to dissolve the polymer.[40] Moreover, in the case of poly-(*R*)-**2**, the presence of a strong electron-withdrawing group, CF_3, should deactivate the donor character of the amide. From these designs, therefore, it is possible to verify the role of the amide group in the stabilization of the nanocomposites of PPA−AgNPs.

PPA copolymers based on poly-(*R*)-**1** that incorporate thiolated comonomers were also prepared but their PPA−AgNP nanocomposites did not show, as expected, the dynamic behavior showed by the parent copolymers (see the Supporting Information and ref 14).

Preparation of Poly-(*R*)-1-AgNP and Poly-(*R*)-2-AgNP Nanocomposites: Dynamic and Aggregation Studies. Poly-(*R*)-**1**-AgNP and poly-(*R*)-**2**-AgNP nanocomposites were prepared by reduction with $NaBH_4$ of two different solutions containing poly-(*R*)-**1**/Ag^+ and poly-(*R*)-**2**/Ag^+ complexes as described below.

As will be seen throughout this discussion, the presence of mono- and divalent metal cations (M^{n+} = Li^+, Na^+, Ag^+, and Ba^{2+}) also plays a fundamental role when describing these nanocomposites. Therefore, from now on, we will use names for the forms "poly-(*R*)-**1**(or **2**)-AgNPs/M^{n+}" when these cations are present and "poly-(*R*)-**1**(or **2**)-AgNPs" when they are not.

Poly-(R)-1-AgNPs/Na^+ Nanocomposite. A methanolic solution (0.5 equiv) of $AgClO_4$ (10 mg·mL^{-1}) was added to a chloroform solution of poly-(*R*)-**1** (0.3 mg·mL^{-1}).

CD studies showed a chiral enhancement of the axially racemic poly-(*R*)-**1** (CD_{380} = 0) toward an *M* helical sense

https://doi.org/10.1021/acs.chemmater.1c00805
Chem. Mater. 2021, 33, 4805−4812

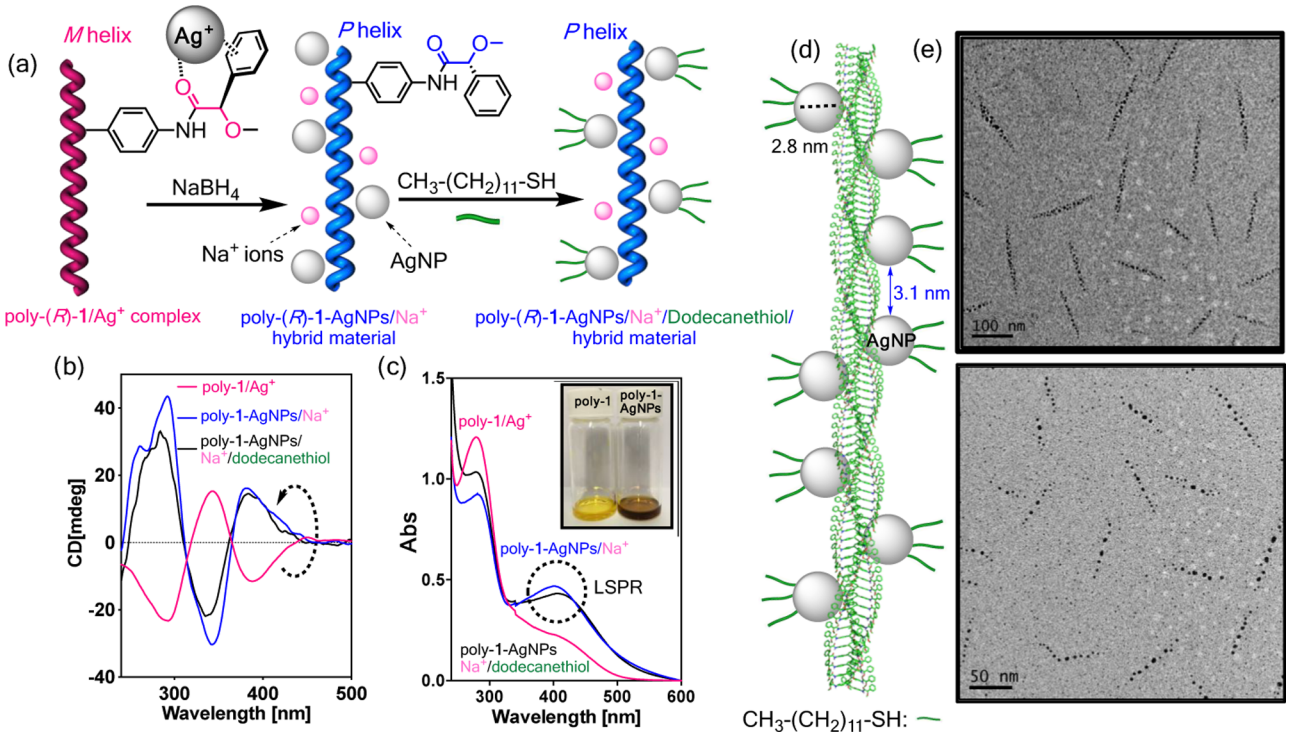

Figure 2. (a) Schematic representation of the *M* helix induction of poly-(*R*)-**1** by complexation with Ag^+ followed by reduction with $NaBH_4$ to form the desired poly-(*R*)-**1**-AgNPs/Na^+ followed by further stabilization with dodecanethiol. (b) CD spectra of poly-(*R*)-**1**/Ag^+, poly-(*R*)-**1**-AgNPs/Na^+, and poly-(*R*)-**1**-AgNPs/Na^+/dodecanethiol. (c) UV−vis spectra for poly-(*R*)-**1**/Ag^+, poly-(*R*)-**1**-AgNPs/Na^+, and poly-(*R*)-**1**-AgNPs/Na^+/dodecanethiol. (d) Molecular model of poly-(*R*)-**1**-AgNPs. (e) Transmission electron microscopy (TEM) images of poly-(*R*)-**1**-AgNPs/Na^+/dodecanethiol.

($CD_{380} < 0$) due to the complexation of poly-(*R*)-**1** with Ag^+ to form the poly-(*R*)-**1**/Ag^+ complex in a 1.0/0.5 mol/mol ratio (Figure 2a,b).[18] Next, 1 equiv of the reducing agent ($NaBH_4$, 1 mg·mL^{-1}, MeOH) was added to the solution mixture. CD studies showed an *M* ($CD_{380} < 0$) to *P* helical inversion ($CD_{380} > 0$) (Figure 2a,b). Simultaneously, the appearance of an LSPR band in the UV−vis spectrum around 404 nm was observed, indicating the formation of spherical AgNPs (Figure 2c). Moreover, Fourier transform infrared (FT-IR) and ^1H NMR studies confirmed the formation of the poly-(*R*)-**1**-AgNPs/Na^+ hybrid material (see the Supporting Information). This nanocomposite showed little stability in solution over time, forming aggregates that were detected by the depletion of the LSPR band (see the Supporting Information, Figure S23). To prevent the aggregation of the poly-(*R*)-**1**-AgNPs/Na^+ nanocomposite and improve its stability in the solution, 1-dodecanethiol was used as a coprotecting agent.

Thus, 0.2 equiv of 1-dodecanethiol was added to a dispersion of poly-(*R*)-**1**-AgNPs/Na^+ immediately after addition of the reducing agent. In these conditions, the poly-(*R*)-**1**-AgNPs/Na^+/dodecanethiol nanocomposite shows an LSPR band at ca. 412 nm, whose intensity does not vary with time, therefore confirming the presence of a stable poly-(*R*)-**1**-AgNPs/Na^+ hybrid material (Figure 2c).

The morphology of the poly-(*R*)-**1**-AgNPs/Na^+/dodecanethiol nanocomposite was studied by electron microscopy studies. To this end, a solution of the poly-(*R*)-**1**-AgNPs/Na^+/dodecanethiol nanocomposite was drop-cast onto a silicon wafer and a carbon grid for scanning (SEM) and transmission electron microscopy (TEM) studies, respectively. The images obtained from these studies showed the presence of small and regularly distributed AgNP nanospheres (2.8 ± 0.6 nm), which are randomly distributed along the helical polymer periphery and separated ca. 3.1 nm, a value that is coincident with the helical pitch of poly-(*R*)-**1** (Figure 2d,e and the Supporting Information, Figures S21 and S25).

Hence, the helical PPA acts as a template by fixing the Ag^+ ions on the amide groups of the polymer. Further reduction of these silver ions to Ag^0 leads to the formation of AgNPs regularly aligned on the polymer.

An interesting effect observed during the formation of the poly-(*R*)-**1**-AgNPs/Na^+ nanocomposite that deserves to be explained is the helical inversion from *M* to *P* produced in poly-(*R*)-**1** when Ag^+ in the poly-(*R*)-**1**/Ag^+ complex is reduced to Ag^0 using $NaBH_4$.

From previous studies, it is known that poly-(*R*)-**1** behaves as axially racemic in $CHCl_3$, a mixture of *P* and *M* helices in equal populations. The addition of perchlorate salts of monovalent metal ions such as Li^+, Na^+, or Ag^+ to a chloroform solution of poly-(*R*)-**1** leads to the formation of a poly-(*R*)-**1**/M^+ complex, where the metal ion coordinates the carbonyl of the anilide group and establishes a cation−π interaction with the aryl ring of the pendant. The strength of the cation−π interactions depends on the nature of the metal cation. For instance, only a few examples of Na^+−π complexes have been published, being known that cation−π interactions with Na^+ are weaker than with Li^+.[41−45]

As a result, an antiperiplanar conformation of the (O−)C—C(=O) bond is fixed in the pendant (Figure 2a), which induces an excess of *M* helical sense in the PPA.[18,38] Nevertheless, in the special case of the poly-(*R*)-**1**/Na^+ complex, it was found that the addition of a donor solvent such as MeOH disrupts the cation−π interaction and promotes the formation of a new chelate between the Na^+ ion and the

https://doi.org/10.1021/acs.chemmater.1c00805
Chem. Mater. 2021, 33, 4805−4812

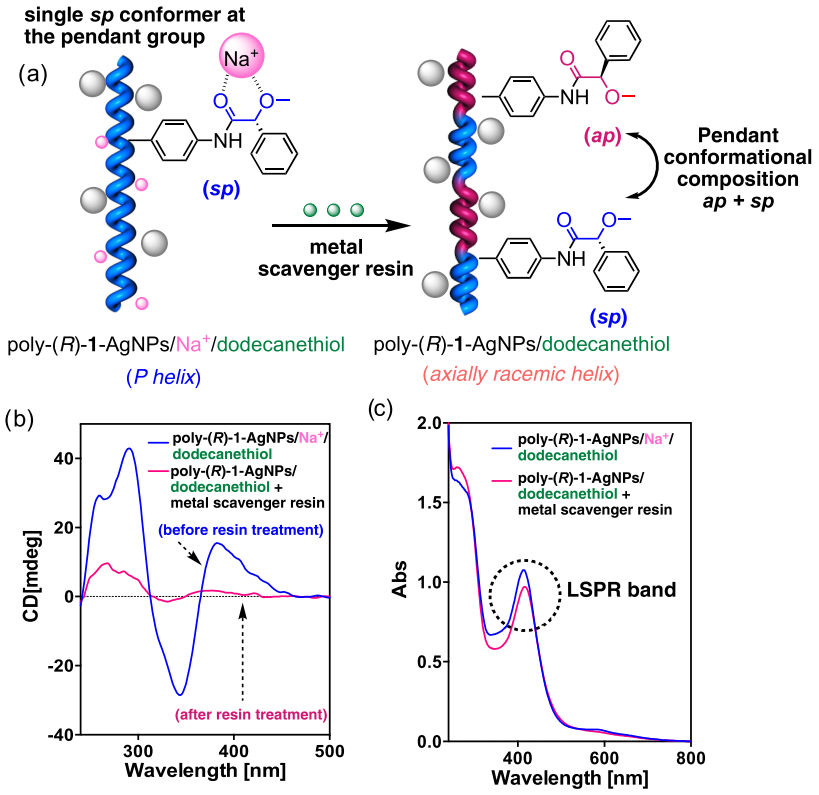

Figure 3. (a) Schematic illustration of the role of Na^+ in the formation of poly-(*R*)-**1**-AgNPs/Na^+ nanocomposites. (b) CD studies of poly-(*R*)-**1**-AgNPs/Na^+ prepared using $NaBH_4$ before and after treatment with a metal scavenger resin and (c) UV−vis studies of a poly-(*R*)-**1**-AgNPs/Na^+ prepared using $NaBH_4$ before and after treatment with a metal scavenger resin.

carbonyl and methoxy groups of the pendant moiety (Figure 3).[41] As a consequence, a synperiplanar conformation of the (O−)C—C(=O) bond is stabilized in the pendant, inducing a *P* helix in the PPA.[41] Therefore, an *M* to *P* helix inversion occurs in the poly-(*R*)-**1**/Na^+ complex through activation/deactivation of the cation−π interaction.[41]

This information suggests that the helix inversion that occurs when poly-(*R*)-**1**/Ag^+ is transformed into poly-(*R*)-**1**-AgNPs/Na^+ may be related to the presence of Na^+ ions introduced with the $NaBH_4$ reducing agent, poly-(*R*)-**1**-AgNPs/Na^+, and not to the AgNPs themselves. Hence, several experiments were carried out to confirm this hypothesis.

Use of Metal Scavenger Resins. The poly-(*R*)-**1**-AgNPs/Na^+/dodecanethiol nanocomposite was dispersed in chloroform (0.3 mg·mL^{-1}), positive CD, *P* helix. The addition of a metal scavenger resin (Quadrapure IDA) produces an axially racemic helix, similar to that observed for poly-(*R*)-**1** when dissolved in chloroform in the absence of metal ions (Figure 3b). UV−vis studies of the poly-(*R*)-**1**-AgNPs/Na^+/dodecanethiol nanocomposite after treatment with the metal scavenger resin show the LSPR band of spherical AgNPs, indicating that the nanocomposite remains unaltered before and after the addition of the scavenger (Figure 3c).

This experiment indicates that the *P* helical sense induced in the poly-(*R*)-**1**-AgNPs/Na^+/dodecanethiol nanocomposite is due to the presence of Na^+ ions from $NaBH_4$, which form complexes with the hybrid material, poly-(*R*)-**1**-AgNPs/Na^+/dodecanethiol. The addition of a metal scavenger resin removes the Na^+ ions from the dispersed nanocomposite, poly-(*R*)-**1**-AgNPs/dodecanethiol hybrid material, which recovers its highly dynamic behavior (equal mixture of *P* and *M* helices) (Figure 3a).

$LiBH_4$ as a Reducing Agent. From previous studies, it is known that the poly-(*R*)-**1**/Na^+ complex can selectively adopt an *M* or *P* helical sense by activation/deactivation of cation−π interactions. In the case of the poly-(*R*)-**1**/Li^+ complex, disruption of the cation−π interaction is not possible, and as a result, only an *M* helix can be induced in that complex (see the Supporting Information, Figure S27).[41]

Thus, when $LiBH_4$ is used as a reducing agent to produce the poly-(*R*)-**1**-AgNPs/Li^+/dodecanethiol nanocomposite, an *M* helix is induced in poly-(*R*)-**1**, opposite to the resulting *P* helix when $NaBH_4$ is used as reducer, poly-(*R*)-**1**-AgNPs/Na^+/dodecanethiol nanocomposite, (see the Supporting Information, Figure S27). The subsequent addition of a metal scavenger resin to trap Li^+ ions produces, as expected, the formation of a macroscopically racemic poly-(*R*)-**1**-AgNPs nanocomposite. This fact clearly indicates that the *P* and *M* helical senses induced in the poly-(*R*)-**1**-AgNPs/Li^+/dodecanethiol hybrid material are due to the Na^+ and Li^+ ions present in $NaBH_4$ and $LiBH_4$ and not due to the presence of AgNPs.

Dynamic Behavior of Poly-(R)-1-AgNPs/Dodecanethiol. The dynamic behavior of axially racemic poly-(*R*)-**1**-AgNPs/dodecanethiol was studied by adding 0.2 equiv of $AgClO_4$ and $Ba(ClO_4)_2$ as sources of monovalent and divalent metal ions, [$AgClO_4$ and $Ba(ClO_4)_2$] = 10 mg·mL^{-1}, MeOH. In both cases, large chiral enhancements were observed toward *M*, poly-(*R*)-**1**-AgNPs/Ag^+/dodecanethiol, and *P*, poly-(*R*)-**1**-AgNPs/Ba^{2+}/dodecanethiol, helices, similar to those obtained for poly-(*R*)-**1**/Ag^+ and poly-(*R*)-**1**/Ba^{2+}, respectively (Figure 4b and the Supporting Information, Figures S32 and S33).

https://doi.org/10.1021/acs.chemmater.1c00805
Chem. Mater. 2021, 33, 4805−4812

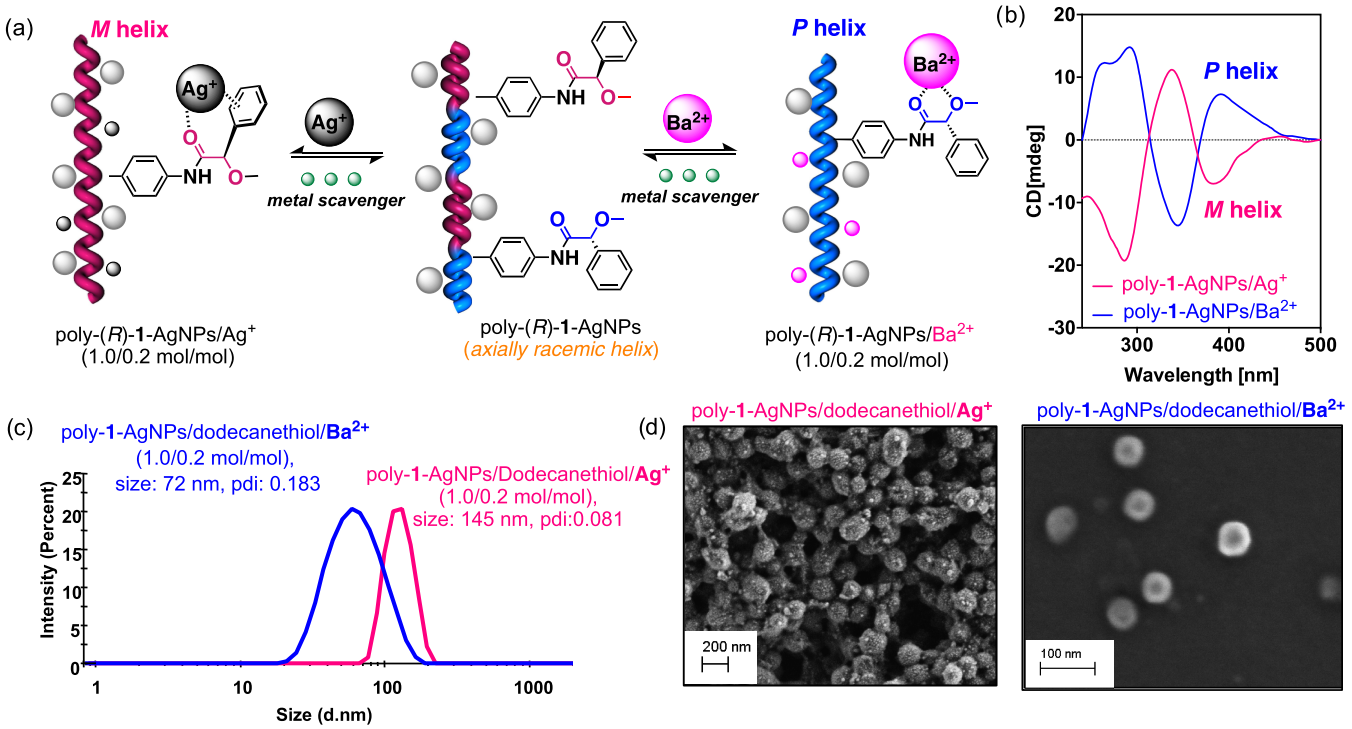

Figure 4. (a) Chiral enhancement of poly-(*R*)-**1**-AgNPs nanocomposites by addition of 0.2 equiv of Ag^+ and Ba^{2+}. (b) CD studies of poly-(*R*)-**1**-AgNPs/Ag^+/dodecanethiol and poly-(*R*)-**1**-AgNPs/Ba^{2+}/dodecanethiol complexes. (c) Dynamic light scattering (DLS) studies of poly-(*R*)-**1**-AgNPs/Ag^+/dodecanethiol and poly-(*R*)-**1**-AgNPs/Ba^{2+}/dodecanethiol complexes. (d) SEM images of poly-(*R*)-1-AgNPs/Ag^+/dodecanethiol and poly-(*R*)-**1**-AgNPs/Ba^{2+}/dodecanethiol nanospheres.

These results indicate that a supramolecular interaction between the metal nanoparticle and the polymer does not affect the dynamic helical behavior of the polymer. They also reveal that poly-(*R*)-**1**-AgNPs/dodecanethiol follows a self-adaptive mechanism, in which AgNPs lodge at different locations in PPA in response to the helical structural changes that the polymer undergoes.

Aggregation Control of Poly-(R)-1-AgNPs/M^{n+}/Dodecanethiol Complexes. The ability of poly-(*R*)-**1**/M^{n+}/dodecanethiol complexes to form nanostructures such as nanospheres[18,38] was tested in the nanocomposite/M^{n+} complex, poly-(*R*)-**1**-AgNPs/M^{n+}, M^{n+} = Ag^+, Ba^{2+} (Figure 4a). Thus, the poly-(*R*)-**1**-AgNPs/dodecanethiol nanocomposite was dispersed in chloroform (0.3 mg·mL^{-1}) and 0.2 equiv of $AgClO_4$ was added to form the poly-(*R*)-**1**-AgNPs/Ag^+/dodecanethiol complex in a 1.0/0.2 mol/mol ratio. DLS and SEM show the formation of stable and low polydispersed nanospheres (size: 163 ± 36 nm) (Figure 4c,d), which are made of helical structures with an *M* helical sense excess (CD_{380} < 0). Interestingly, it is possible to distinguish the AgNP nanoparticles embedded in the nanospheres from the SEM images (Figure 4d).

Similar experiments were carried for poly-(*R*)-**1**-AgNPs/Ba^{2+}/dodecanethiol in a 1.0/0.2 mol/mol ratio that led to the formation of low polydispersed nanospheres (size: 61 ± 21 nm) with opposite macroscopic chirality (*P* helices, CD_{380} > 0) (see Figure 4c,d and the Supporting Information, Figures S32 and S33).

Poly-(R)-2-AgNPs/Dodecanethiol Nanocomposite. Poly-(*R*)-**2**-AgNPs/dodecanethiol was prepared using poly-(*R*)-**2** as a template and resorting to the same methodology developed to prepare the poly-(*R*)-**1**-AgNPs/dodecanethiol nanocomposite. This polymer adopted an *M* helix (CD_{380} < 0) once was dissolved in chloroform (Figure 5a–c).[40] Ulterior addition of a methanolic solution of 0.5 equiv of $AgClO_4$ (10 mg·mL^{-1}) generated the poly-(*R*)-**2**/Ag^+ complex by coordination of the Ag^+ ions to the carbonyl group of the pendant, although no helical changes were observed in poly-(*R*)-**2** (CD_{380} < 0) (Figure 5a–c). Next, the formation of the poly-(*R*)-**2**-AgNP/dodecanethiol nanocomposite was achieved by adding $NaBH_4$ as a reducing agent (see the Supporting Information for a full structural characterization). TEM studies of the poly-(*R*)-**2**-AgNP/dodecanethiol nanocomposite indicated the role of the amide group in the stabilization of AgNPs. In this case, the presence of a strong electron-withdrawing group ($-CF_3$) in poly-(*R*)-**2** diminishes the donor capacity of the amide function. This fact has a great effect on the stabilization of AgNPs, which leads to the formation of irregular, polydispersed, and randomly distributed AgNPs within the poly-(*R*)-**2**-AgNP/dodecanethiol nanocomposite (Figure 5d).

CONCLUSIONS

A novel approach to obtain PPA–AgNP nanocomposites without altering the dynamic behavior of the parent polymer is described.

Weak amide–AgNP supramolecular interactions are used to prepare chiral dynamic nanocomposites. To perform these studies, poly-(*R*)-**1**, bearing 4-anilide of (*R*)-*α*-methoxy-*α*-phenylacetic acid was chosen as a protecting agent. First, a poly-(*R*)-**1**/Ag^+ complex is formed in a 1.0/0.5 mol/mol ratio, which is further reduced to the poly-(*R*)-**1**/AgNPs/Na^+/dodecanethiol nanocomposite using $NaBH_4$ as a reducing agent. TEM studies of the nanocomposite show that the AgNPs are regularly distributed along the polymer chain. Poly-(*R*)-**1** acts as a template by placing the AgNPs at fixed

https://doi.org/10.1021/acs.chemmater.1c00805
Chem. Mater. 2021, 33, 4805–4812

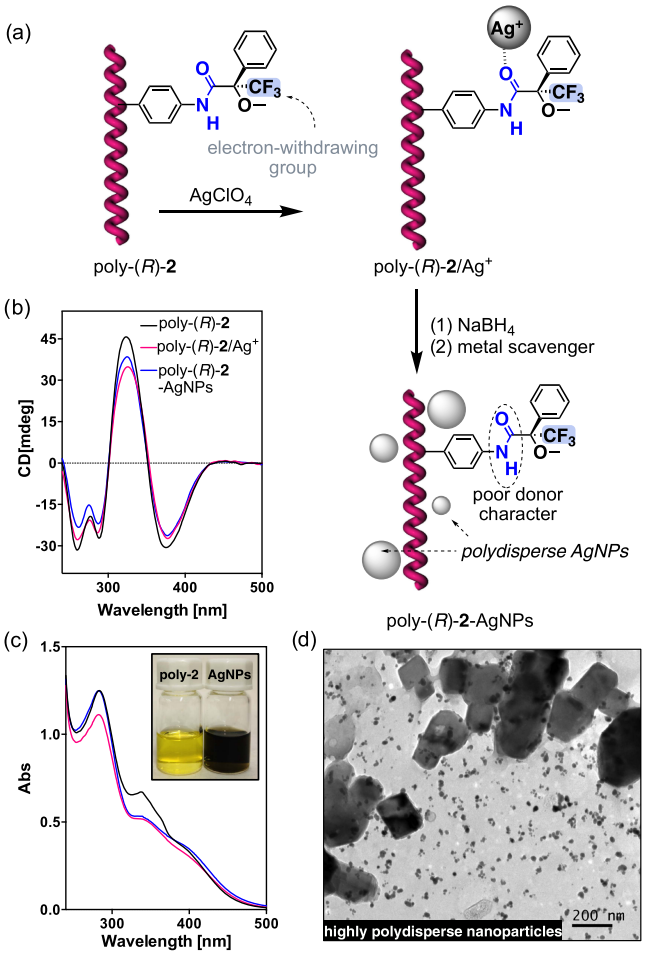

Figure 5. (a) Schematic illustration of poly-(*R*)-**2**-AgNPs/dodecanethiol nanocomposite formation. (b) CD studies of poly-(*R*)-**2**, poly-(*R*)-**2**/Ag^+ (1.0/0.5 mol/mol) and poly-(*R*)-**2**-AgNPs. (c) UV−vis studies of poly-(*R*)-**2**, poly-(*R*)-**2**/Ag^+ (1.0/0.5 mol/mol) and poly-(*R*)-**2**-AgNPs. (d) TEM images of poly-(*R*)-**2**-AgNPs/dodecanethiol.

distances of 3.1 nm, which corresponds to the helical pitch of poly-(*R*)-**1**. Stimuli-responsive studies show that the poly-(*R*)-**1**/AgNPs/dodecanethiol nanocomposite responds to monovalent and divalent metal ions just like the parent polymer, poly-(*R*)-**1**, does. Hence, a *P* helix is induced by monovalent metal ions, while an *M* helix is fixed when divalent metal ions are added to a dispersion of the hybrid material. Moreover, during these studies, the ability of the poly-(*R*)-**1**/AgNPs/M^{n+}/dodecanethiol nanocomposite to form other nanostructures such as nanospheres was also demonstrated.

EXPERIMENTAL SECTION

Chemicals. Commercially available chemicals were used as delivered. Solvents were purchased of reagent grade and distilled if necessary. Anhydrous solvents were either purchased as ultradry solvents from Acros Organics or received from a solvent purification system. For the coupling and polymerization reactions, dry tetrahydrofuran (THF) was obtained from an MBRAUN SPS 800 solvent purification system. Water was purified by a Millipore water purification system. Coupling reagents (2-(7-aza-1*H*-benzotriazole-1-yl)-1,1,3,3-tetramethyluronium hexafluorophosphate) (HATU), 1-hydroxy-7-azabenzotriazole (HOAT), 4- ethynylbenzoic acid, and 4-ethynylaniline were purchased from AnaSpec Inc. (*R*)-α-Methoxyphenylacetic acid, (*R*)-α-methoxy-α-trifluorophenylacetic acid, oxalyl choride, rhodium norbornadiene chloride dimer $\{[Rh(nbd)Cl]_2\}$, diisopropyltriethylamine (DIEA), triethylamine (TEA, 99%), dodecanethiol, sodium borohydride ($NaBH_4$), silver perchlorate ($AgClO_4$), and barium perchlorate $[Ba(ClO_4)_2]$ were purchased from Sigma-Aldrich.

Instrumentation and Characterization. NMR experiments were carried out in a Varian Inova 300 (300 MHz resonance 1H). Size exclusion chromatography studies were performed on an Alliance 2695 HPLC (Waters) liquid chromatography system equipped with a UV 2489 detector (Waters). The samples were eluted by three Phenogel columns connected to each other with stationary phases of 10^3, 10^4, and 10^5 Å and packed with a solid support of a cross-linked styrene and *p*-divinylbenzene copolymer. CD and UV measurements were performed in a Jasco-720 spectropolarimeter and a Jasco-730 spectrophotometer, respectively, at a nanocomposite concentration of 0.3 mg·mL^{-1}. FT-IR measurements were carried out on a Bruker IFS-66v. DLS studies were performed on a Nano-ZS 90 (Malvern) equipped with a He−Ne laser (l = 633 nm) under a scattering angle of 173°. The samples were maintained at the designed temperature for 5 min before testing. DLS measurements were carried out in all cases at 0.3 mg·mL^{-1}. SEM samples were performed on a LEO-435VP electron microscope. SEM measurements were performed on a LEO-435VP electron microscope equipped with an energy-dispersive X-ray (EDX) spectrometer. TEM measurements were performed on a JEOL JEM 2010 and 200 kV as a voltage. To study the nanocomposite or the nanospheres, the same protocol was used. A dispersion of the nanocomposite or the nanospheres at a concentration of 0.3 mg·mL^{-1} was drop-casted onto a silicon wafer chip and allowed to dry at rt for 12 h for SEM studies, while in the case of TEM studies, the dispersed materials were drop-casted onto a carbon chip and allowed to dry at rt for 12.h.

ASSOCIATED CONTENT

Supporting Information

The Supporting Information is available free of charge at https://pubs.acs.org/doi/10.1021/acs.chemmater.1c00805.

Materials and methods; synthesis of monomer M1; synthesis of monomer M2; synthesis of polymers poly-(*R*)-1 and poly-(*R*)-2; CD and UV−vis studies of poly-(*R*)-2 with monovalent and divalent metal ions; general procedure of synthesis of poly-1-AgNPs and poly-(*R*)-2-AgNPs; ^1H NMR of poly-1-AgNPs; FT-IR studies of poly-(*R*)-1-AgNPs and poly-(*R*)-2-AgNPs; synthesis of poly-1-AgNPs in different solvents; CD and UV−vis studies of poly-1-AgNPs/metal ion interactions; microscopy studies of poly-1-AgNPs: SEM and TEM images; the stability of poly-(*R*)-1-AgNPs with time; stabilization of poly-(*R*)-1-AgNPs using dodecanethiol; microscopy studies of poly-2-AgNPs: TEM images; formation of poly-(*R*)-1-AgNPs using $LiBH_4$; the effect of $NaBH_4$ in the helical sense of poly-(*R*)-1-AgNPs; the role of Na^+ cations in the helicity of poly-(*R*)-1-AgNPs, experiments with metal scavenger resins; formation of chiral nanospheres using poly-(*R*)-1-AgNPs and monovalent and divalent metal ions; control studies: "enantiomer comparison"; control studies: "thiol linkage" poly-$[(R)\text{-}1_r\text{-}co\text{-}3_{1-r}]$; chiral enhancement and reversibility of the process with resin metal scavengers in the presence of silver nanoparticles; and references (PDF)

AUTHOR INFORMATION

Corresponding Author

Félix Freire − *Centro Singular de investigación en Química Biolóxica e Materiais Moleculares (CiQUS) and Departamento de Química Orgánica, Universidade de Santiago de Compostela, E-15782 Santiago de Compostela,*

https://doi.org/10.1021/acs.chemmater.1c00805
Chem. Mater. 2021, 33, 4805−4812

Spain; orcid.org/0000-0002-2672-5830;
Email: felix.freire@usc.es

Authors

Manuel Núñez-Martínez − *Centro Singular de investigación en Química Biolóxica e Materiais Moleculares (CiQUS) and Departamento de Química Orgánica, Universidade de Santiago de Compostela, E-15782 Santiago de Compostela, Spain;* orcid.org/0000-0003-2715-0722

Sandra Arias − *Centro Singular de investigación en Química Biolóxica e Materiais Moleculares (CiQUS) and Departamento de Química Orgánica, Universidade de Santiago de Compostela, E-15782 Santiago de Compostela, Spain*

Emilio Quiñoá − *Centro Singular de investigación en Química Biolóxica e Materiais Moleculares (CiQUS) and Departamento de Química Orgánica, Universidade de Santiago de Compostela, E-15782 Santiago de Compostela, Spain;* orcid.org/0000-0003-3019-3408

Ricardo Riguera − *Centro Singular de investigación en Química Biolóxica e Materiais Moleculares (CiQUS) and Departamento de Química Orgánica, Universidade de Santiago de Compostela, E-15782 Santiago de Compostela, Spain*

Complete contact information is available at:
https://pubs.acs.org/10.1021/acs.chemmater.1c00805

Notes

The authors declare no competing financial interest.

■ ACKNOWLEDGMENTS

The authors thank Servicio de Microscopía Electrónica (RIAIDT, USC). Financial support from AEI (PID2019-109733GB-I00), Xunta de Galicia ED431C 2018/30, Centro Singular de Investigación de Galicia acreditación 2019−2022, ED431G 2019/03, Beca Leonardo a Investigadores y Creadores Culturales 2020 de la Fundación BBVA, and the European Regional Development Fund (ERDF) is gratefully acknowledged. N.-M. thanks MICINN for a FPI contract (BES-2016-078107).

■ REFERENCES

(1) Pigliacelli, C.; Sánchez-Fernández, R.; D. García, M.; Peinador, C.; Pazos, E. Self-assembled peptide-inorganic nanoparticle superstrucutres: from component design to applications. *Chem. Commun.* **2020**, *56*, 8000−8014.
(2) Zheng, G.; Bao, Z.; Pérez-Juste, J.; Ruolan, D.; Liu, W.; Dai, J.; Zhang, W.; Lee, L.; Wong, K-Y. Tuning the Morphology and Chiroptical Properties of Discrete Gold Nanorods with Amino Acids. *Angew. Chem., Int. Ed.* **2018**, *57*, 16452−16457.
(3) Jaque, D.; Martínez Maestro, L.; del Rosal, B.; Haro-Gonzalez, P.; Benayas, A.; Plaza, J. L.; Martín Rodriguez, E.; García Solé, J. Nanoparticles for photothermal therapies. *Nanoscale* **2014**, *6*, 9494−9530.
(4) Liu, J.; Lu, Y. Preparation of aptamer-linked gold nanoparticle purple aggregates for colorimetric sensing of analytes. *Nat. Protoc.* **2006**, *1*, 246−252.
(5) Dreaden, E.; Alkilany, A.; Huang, X.; Murphy, C.; El-Sayed, M. The golden age: gold nanoparticles for biomedicine. *Chem. Soc. Rev.* **2012**, *41*, 2740−2779.
(6) Zhang, S.; Geryak, R.; Geldmeier, J.; Kim, S.; Tsukruk, V. Synthesis, Assembly, and Applications of Hybrid Nanostructures for Biosensing. *Chem. Rev.* **2017**, *117*, 12942−13038.
(7) Fleischmann, M.; Hendra, P. J.; McQuillan, A. J. Raman spectra of pyridine adsorbed at a silver electrode. *Chem. Phys. Lett.* **1974**, *26*, 163−166.
(8) Kvítek, L.; Prucek, R.; Panácek, A.; Novotny, A.; Hrbác, J.; Zoboril, R. The influence of complexing agent concentration on particle size in the process of SERS active silver colloid synthesis. *J. Mater. Chem.* **2005**, *15*, 1099−1105.
(9) Faulds, K.; Ewen Smith, W.; Graham, D. Evaluation of Surface-Enhanced Resonance Raman Scattering for Quantitative DNA Analysis. *Anal. Chem.* **2004**, *76*, 412−417.
(10) Lu, X.; Song, D.-P.; Ribbe, A.; Watkings, J. Chiral Arrangements of Au Nanoparticles with Prescribed Handedness Templated by Helical Pores in Block Copolymer Films. *Macromolecules* **2017**, *50*, 5293−5300.
(11) Lin, Y.-L.; Chu, J.-L.; Lu, H.-J.; Liu, N.; Wu, Z.-Q. Facile Synthesis of Optically Active and Magnetic Nanoparticles Carrying Helical Poly(phenyl isocyanide) Arms and Their Application in Enantioseletive Crysallization. *Macromol. Rapid Commun.* **2018**, *39*, No. 1700685.
(12) Zhang, C.; Song, C.; Yang, W.; Deng, J. Au@poly-(propargylamide) Nanoparticles: Preparation and Chiral recognition. *Macromol. Rapid Commun.* **2013**, *34*, 1319−1324.
(13) Freire, F.; Quiñoá, E.; Riguera, R. Chiral nanostructure in polymers under different deposition conditions observed using atomic force microscopy of monolayers: poly(phenylacetylene)s as a case study. *Chem. Commun.* **2017**, *53*, 481−492.
(14) Bergueiro, J.; Nuñez-Martínez, M.; Arias, S.; Quiñoá, E.; Riguera, R.; Freire, F. Chiral gold−PPA nanocomposites with tunable helical sense and morphology. *Nanoscale Horiz.* **2020**, *5*, 495−500.
(15) Van Leeuwen, T.; Heideman, H. G.; Zhao, D.; Wezenberg, S. J.; Feringa, B. L. *In situ* control of polymer helicity with a non-covalently bound photoresponsive molecular motor dopant. *Chem. Commun.* **2017**, *53*, 6393−6396.
(16) Wang, S.; Chen, J.; Feng, X.; Shi, G.; Zhang, J.; Wan, X. Conformation Shift Switches the Chiral Amplification of Helical Copoly(phenylacetylene)s from Abnormal to Normal "Sergeants-and-Soldiers" Effect. *Macromolecules* **2017**, *50*, 4610−4615.
(17) Freire, F.; Quiñoá, E.; Riguera, R. Supramolecular Assemblies from Poly(phenylacetylene)s. *Chem. Rev.* **2016**, *116*, 1242−1271.
(18) Freire, F.; Seco, J. M.; Quiñoá, E.; Riguera, R. Helical Polymer−Metal Complexes: The Role of Metal Ions on the Helicity and the Supramolecular Architecture of Poly(phenylacetylene)s. *Adv. Polym. Sci.* **2013**, *262*, 123−140.
(19) Yashima, E. Synthesis and structure determination of helical polymers. *Polym. J.* **2010**, *42*, 3−16.
(20) Yashima, E.; Maeda, K. Chirality-Responsive Helical Polymers. *Macromolecules* **2008**, *41*, 3−12.
(21) Percec, V.; Rudick, J. G.; Peterca, M.; Heiney, P. A. Nanomechanical Function from Self-Organizable Dendronized Helical Polyphenylacetylenes. *J. Am. Chem. Soc.* **2008**, *130*, 7503−7508.
(22) Li, Y.-X.; Xu, L.; Kang, S.-M.; Zhou, L.i.; Liu, N.; Wu, Z.-Q. Helicity- and Molecular-Weight-Driven Self-Sorting and Assembly of Helical Polymers towards Two-Dimensional Smectic Architectures and Selectively Adhesive Gels. *Angew. Chem., Int. Ed.* **2021**, *60*, 7174−7179.
(23) Zhou, L.; Chong-Long, L.; Run-Tan, G.; Shu-Ming, K.; Lei, X.; Xun-Hui, X.; Na, L.; Zong-Quan, W. Highly Regioselective and Helix-Sense Selective Living Polymerization of Phenyl and Alkoxyallene Using Chiral Nickel(II) Catalysts. *Macromolecules* **2021**, *54*, 679−686.
(24) Zhou, L.; Xun-Hui, X.; Zhi-Qiang, J.; Lei, X.; Ben-Fa, C.; Na, L.; Zong-Quan, W. Selective Synthesis of Single-Handed Helical Polymers from Achiral Monomer and a Mechanism Study on Helix-Sense-Selective Polymerization. *Angew. Chem., Int. Ed.* **2021**, *60*, 806−812.
(25) Pastoriza-Santos, I.; Liz-Marzán, L. M. N,N-Dimethylformamide as a Reaction Medium for Metal Nanoparticle Synthesis. *Adv. Funct. Mater.* **2009**, *19*, 679−688.

(26) Huang, H.; Ni, X. P.; Loy, G. L.; Chew, C. H.; Tan, K. L.; Loh, F. C.; Deng, J. F.; Xu, G. Q. Nanoparticles in Poly(*N*-vinylpyrrolidone). *Langmuir* **1996**, *12*, 909−912.
(27) Zhang, Z.; Zhao, B.; Hu, L. PVP protective mechanism of ultrafine silver powder synthesized by chemical reduction processes. *J. Solid State Chem.* **1996**, *121*, 105.
(28) Arias, S.; Núñez-Martinez, M.; Quiñoá, E.; Riguera, R.; Freire, F. A general route to chiral nanostructures from helical polymers: *P*/*M* switch via dynamic metal coordination. *Polym. Chem.* **2017**, *8*, 3740−3745.
(29) Rodríguez, R.; Arias, S.; Quiñoá, E.; Riguera, R.; Freire, F. The role of the secondary structure of helical poly(phenylacetylene)s in the formation of nanoparticles from polymer−metal complexes (HPMCs). *Nanoscale* **2017**, *9*, 17752−17757.
(30) Suárez-Picado, E.; Quiñoá, E.; Riguera, R.; Freire, F. Poly(phenylacetylene) Amines: A General Route to Water-Soluble Helical Polyamines. *Chem. Mater.* **2018**, *30*, 6908−6914.
(31) Rodríguez, R.; Suárez-Picado, E.; Quiñoá, E.; Riguera, R.; Freire, F. Stimuli-responsive Macromolecular Gear: Interlocking Dynamic Helical Polymers with Foldamers. *Angew. Chem., Int. Ed.* **2020**, *59*, 8616−8622.
(32) Suárez-Picado, E.; Quiñoá, E.; Riguera, R.; Freire, F. Chiral Overpass Induction in Dynamic Helical Polymers Bearing Pendant Groups with Two Chiral Centers. *Angew. Chem., Int. Ed.* **2020**, *59*, 4537−4543.
(33) Fernández, Z.; Fernández, B.; Quiñoá, E.; Riguera, R.; Freire, F. Chiral Information Harvesting in Helical Poly(acetylene) Derivatives Using Oligo(p-phenyleneethynylene)s as Spacers. *Chem. Sci.* **2020**, *11*, 7182−7187.
(34) Rodríguez, R.; Quiñoá, E.; Riguera, R.; Freire, F. Multistate Chiroptical Switch Triggered by Stimuli-Responsive Chiral Teleinduction. *Chem. Mater.* **2018**, *30*, 2493−2497.
(35) Rodríguez, R.; Quiñoá, E.; Riguera, R.; Freire, F. Architecture of Chiral Poly(phenyl acetylene)s: From Compressed/Highly Dynamic to Stretched/Quasi-Static Helices. *J. Am. Chem. Soc.* **2016**, *138*, 9620−9628.
(36) Fernández, B.; Rodríguez, R.; Rizzo, A.; Quiñoá, E.; Riguera, R.; Freire, F. Predicting the Helical Sense of Poly(phenylacetylene)s from their Electron Circular Dichroism Spectra. *Angew. Chem., Int. Ed.* **2018**, *57*, 3666−3670.
(37) Fernández, B.; Rodríguez, R.; Quiñoá, E.; Riguera, R.; Freire, F. Decoding the ECD Spectra of Poly(phenylacetylene)s: Structural Significance. *ACS Omega* **2019**, *4*, 5233−5240.
(38) Freire, F.; Seco, J. M.; Quiñoá, E.; Riguera, R. Nanospheres with Tunable Size and Chirality from Helical Polymer−Metal Complexes. *J. Am. Chem. Soc.* **2012**, *134*, 19374−19383.
(39) Arias, S.; Núñez-Martinez, M.; Quiñoá, E.; Riguera, R.; Freire, F. Simultaneous Adjustment of Size and Helical Sense of Chiral Nanospheres and Nanotubes Derived from an Axially Racemic Poly(phenylacetylene). *Small* **2016**, *13*, No. 1602398.
(40) Leiras, S.; Freire, F.; Seco, J. M.; Quiñoá, E.; Riguera, R. Controlled modulation of the helical sense and the elongation of poly(phenylacetylene)s by polar and donor effect. *Chem. Sci.* **2013**, *4*, 2735−2743.
(41) Arias, S.; Freire, F.; Quiñoá, E.; Riguera, R. The leading role of cation−π interactions in polymer chemistry: the control of the helical sense in solution. *Polym. Chem.* **2015**, *6*, 4725−4733.
(42) Wu, G.; Terskikh, V. A. Multinuclear Solid-State NMR Study of Alkali Metal Ions in Tetraphenylborate Salts, M[BPh4] (M = Na, K, Rb and Cs): What Is the NMR Signature of Cation−π Interactions? *J. Phys. Chem. A* **2008**, *112*, 10359−10364.
(43) Widdifield, C. M.; Tang, J. A.; Macdonald, C. L. B.; Schurko, R. W. Investigation of Structure and Dynamics in the Sodium Metallocenes CpNa-THF via Solid-State NMR, X-Ray Diffraction and Computacional Modelling. *Magn. Reson. Chem.* **2007**, *45*, S116−S128.
(44) Widdifield, C. M.; Schurko, R. W. A Solid-State ^{39}K and ^{13}C NMR Study of Polymeric Potassium Metallocenes. *J. Phys. Chem. A* **2005**, *109*, 6865−6876.
(45) Willans, M. J.; Schurko, R. W. A Solid-State NMR and ab Initio Study of Sodium Metallocenes. *J. Phys. Chem. B* **2003**, *107*, 5144−5161.

https://doi.org/10.1021/acs.chemmater.1c00805
Chem. Mater. 2021, 33, 4805−4812